TU Delft

Delft University of Technology

A compliant Continuously Variable Transmission (CVT)

Amoozandeh Nobaveh, Ali; Herder, Just L.; Radaelli, Giuseppe

DOI
10.1016/j.mechmachtheory.2023.105281

Publication date
2023

Document Version
Final published version

Published in
Mechanism and Machine Theory

Citation (APA)
Amoozandeh Nobaveh, A., Herder, J. L., & Radaelli, G. (2023). A compliant Continuously Variable Transmission (CVT). *Mechanism and Machine Theory*, *184*, Article 105281. https://doi.org/10.1016/j.mechmachtheory.2023.105281

Important note
To cite this publication, please use the final published version (if applicable).
Please check the document version above.

Copyright
Other than for strictly personal use, it is not permitted to download, forward or distribute the text or part of it, without the consent of the author(s) and/or copyright holder(s), unless the work is under an open content license such as Creative Commons.

Takedown policy
Please contact us and provide details if you believe this document breaches copyrights.
We will remove access to the work immediately and investigate your claim.

This work is downloaded from Delft University of Technology.
For technical reasons the number of authors shown on this cover page is limited to a maximum of 10.

Mechanism and Machine Theory 184 (2023) 105281

Contents lists available at ScienceDirect

Mechanism and Machine Theory

journal homepage: www.elsevier.com/locate/mechmt

Research paper

A compliant Continuously Variable Transmission (CVT)

Ali Amoozandeh Nobaveh *, Just L. Herder, Giuseppe Radaelli

Precision and Microsystems Engineering Department, Delft University of Technology, 2628CD, Delft, The Netherlands

ARTICLE INFO

Keywords:
Continuously Variable Transmission (CVT)
Compliant mechanism
Warping
Twisting beams

ABSTRACT

Continuously Variable Transmissions (CVT) can serve as subsystems for a variety of machineries and robotic systems. A compliant CVT mechanism based on the warping of twisting beams is presented here. The design works based on the demonstrated fact that the twist on one side of a beam can be transferred via sectional warping and propagate across a rotational constraint in the middle of the beam to create a reverse twist on the opposite side. In the proposed compliant CVT the transmission ratio is dependent on the position of the middle rotational constraint which can vary in a continuous range. We have demonstrated this concept and its relation to the twisting beam's warping constant, as well as its functionality for different transmission ratios of 1:4 to 4:1. An analytical model as well as a Finite Element Analysis (FEA) and experiments are employed to characterize and verify the concept and its relation to the warping constant.

1. Introduction

A transmission mechanism is generally a complex, multi-element system. When a continuously variable transmission (CVT) ratio is required, an additional level of complexity might be anticipated. There are several designs for CVT systems, including half and full toroidal CVTs [1], magnetic CVTs [2], and belt- or chain- type CVTs. Designs of the latter type, which is the largest group of known CVTs, utilize two pulleys with variable diameters coupled to one another with a belt or chain [3].

Considering applications requiring light-weight mechanisms like aerospace engineering and wearable robots, using these conventional systems is not viable as they are rather bulky and complex. Also, for small-scale applications, such as sensors or micro robots, these conventional systems are inadequate because of fabrication and assembly problems. Apart from the fact that these mechanisms operate on the basis of contacts between numerous connected elements, which introduces inherent problems such as backlash and other contact-related errors that can reduce the applicability of these conventional variable transmission solutions for applications such as MEMS and micro manufacturing, clean (room) applications i.e. optics and extreme precision [4].

A compliant transmission mechanism is capable of resolving several of the concerns listed above. Due to the fact that these mechanisms operate via elastic deformation of elements rather than contact, issues such as backlash are not present. Additionally, these systems are predominantly monolithic, light-weight and easily fabricable. As a result, a compliant CVT can be used to construct devices such as tiny aerial robots [5], watch oscillators [6], and precision systems such as sensors, or any other application that does not require a full cycle rotation like walking mechanisms for humanoid robots [7,8] or motion transferring for wearable robots [9].

Numerous examples exist of compliant transmission mechanisms [10–12]. However, these compliant transmission systems are mainly planar and were designed by substituting rigid body mechanism joints by compliant parts. As a result, the most of these mechanisms require a very large design area to accommodate the links, and in the majority of situations, linkages can only imply a fix transmission ratio. There are fewer instances of systems that allow for variable transmission ratios, but still in those designs, a reconfiguration of the whole mechanism is required in order to change the transmission ratio, which makes them even less space

* Corresponding author.
E-mail address: a.amoozandehnobaveh@tudelft.nl (A. Amoozandeh Nobaveh).

https://doi.org/10.1016/j.mechmachtheory.2023.105281
Received 14 October 2022; Received in revised form 31 January 2023; Accepted 31 January 2023
Available online 14 February 2023
0094-114X/© 2023 The Author(s). Published by Elsevier Ltd. This is an open access article under the CC BY license (http://creativecommons.org/licenses/by/4.0/).

Nomenclature

λ	Distance between the mid constraint and the input ring.
t	Thickness of the beam webs and flanges.
w_f	Width of the beam flanges.
w_w	Width of the beam webs.
θ	Twist angle of each section of the beam.
φ	Rotation of each section along the beam.
B	Bimoment.
C	A point in the center of the beam.
E	Elastic modulus.
G	Shear modulus.
I_w	Warping constant.
J	St. Venant torsional constant.
L	Length of the beam.
m	Distributed torsion moment along the beam.
M_t	The torsion moment.
x, y, z	Longitudinal, vertical and horizontal directions.

efficient [13,14]. There are another type of these compliant transmissions in literature which can only switch between specified ratios; in other words, they are incapable of continuously covering a range of transmission ratios [15]. Apart from that, the aforementioned planar techniques were primarily created for translation to translation transmission.

To achieve rotation to rotation compliant transmission mechanisms, spatial compliant elements such as twisting beams can be used. Earlier, such an element was employed to morph shapes [16], and also for some compliant revolute joints [17,18], where the bending to torsion stiffness ratio of the beam is crucial for representing joint-like behavior. Strategies such as balancing and prestressing are proposed to further increase this ratio for the joint functionality purposes. However, in non of these compliant twisting elements, designers looked at the possibility of using them as transmissions.

In this work, we use warping as an intrinsic property of a beam with an open thin-walled section, to obtain rotation–rotation transmission. Warping is usually regarded as an undesirable behavior, and designers try to minimize or avoid it. There are only a few applications, e.g. adjusting the effective angles of airplane wings [19], that take advantage of this principle. Warping, or in another words out of plane deformation of cross-sections, can be very effective as it causes axial displacements in a warpable beam. These axial displacements can propagate across an intermediate rotational constraint and cause exceptional effects like twist coupling along the beam, which can be considered a method to transmit the rotation between sides of a warpable beam. The transmission of warping in thin-walled structures is a well-established topic in structural engineering and there are several papers on characterization and possibly avoiding its propagation in the whole structure [20–22]. However, using this warping behavior to achieve a mechanism has only been proposed by the authors as a compliant differential mechanism with a one to one ratio [9,23].

The purpose of this paper is to present a concept for a compliant CVT mechanism that operates by twisting warpable beams. It is demonstrated that the rotation of one beam side can be transmitted by warping along the beam and passing across a rotational constraint in the middle of the beam to cause the opposite side to rotate in reverse. The ratio of the rotation angles at the input and output sides is dependent on the location of the intermediate rotational constraint. As a result, it is demonstrated that by repositioning the middle constraint a continuously variable transmission can be created. We have established and validated this concept using an analytical solution, finite element analysis (FEA) and experiments on the beam prototypes with different warping constants in order to demonstrate the effect of warping on this transmission behavior.

The paper is structured as follows. In Section 2, the concept, and the reasoning behind the captured behavior are introduced. The effective design parameters together with the details of the analytical solution, the FEA and the experimental setup are elaborated in Section 3. In Section 4 the results for all beams and from different methods are shown. A discussion on the validity of the concept and the results, beside possible applications and improvements are given in Section 5. Finally, a brief overview of the achievements and possible applications are stated in Section 6.

2. Concept overview

When a beam with a high warping constant is loaded in torsion, the cross-sections deform in the axial direction of the beam. In other words plane cross-sections are not planar anymore (Fig. 1) [24]. These warping induced axial deformations can propagate along the beam length. Therefore, the rotational constraint perpendicular to the beam's length (fork support) cannot block them. This means that by rotating one side of the beam, they form and transfer the sectional torsion across the rotational constraint and bring it to the other side. This behavior results in a reverse rotation of the output of the beam compared to the input. Here, this principle is used as a transmission and inversion between input and output. The schematic of the mechanism and the warping-induced displacements are shown in Fig. 1.

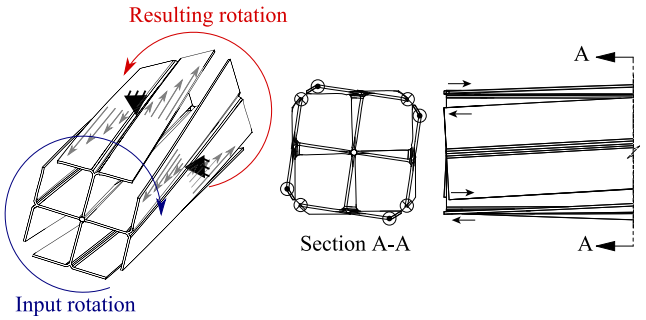

Fig. 1. The working principle of the compliant CVT based on the warping of twisting beams. The axial displacements of the beam flanges, which are caused by the beam warping are also shown with vectors.

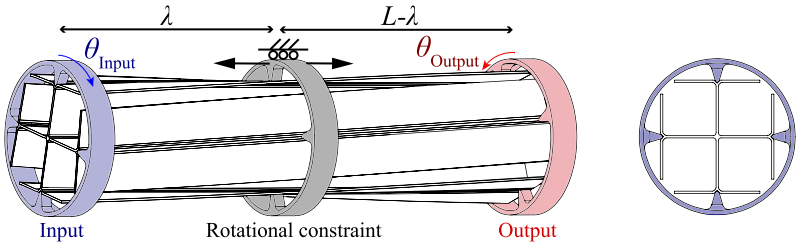

Fig. 2. The input ring (blue), sliding rotational constraint ring (gray), and output ring (red) where rotations and constraints are exerted on the beams by prismatic grooves along the four web tips. The distance between the middle constraints and the beam's sides, which specifies the transmission ratio, are also shown. (For interpretation of the references to color in this figure legend, the reader is referred to the web version of this article.)

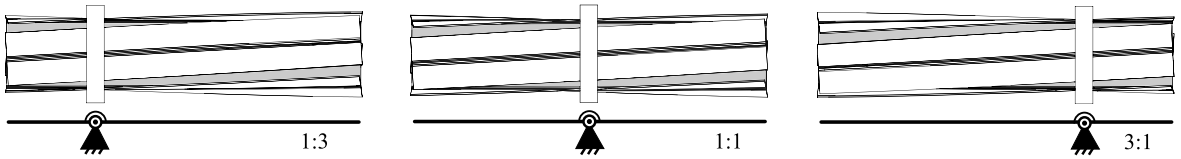

Fig. 3. The comparison between the presented concept, when there is no load at output, and a lever mechanism.

In an ideal case for a twisting beam with high warping constant, if there are no restrains for the warping, a uniform torsion along the beam will form upon a rotation at the input [24], as shown in Fig. 2. This uniform torsion results in a constant twist angle along the whole beam. At the same time, the presence of the prismatic mid-beam rotational constraint (the gray ring) leads to a zero twist angle for this middle cross-section. Therefore, assuming a constant twist angle along the beam, the ratio between output twist angle θ_{Out} (red ring) to input twist angle θ_{In} (blue ring) in an ideal case is equal to the ratio of the distance between mid constraint to input ring λ, over the distance of the mid constraint to the output ring $L-\lambda$ (Fig. 2):

$$\frac{\theta_{\text{Out}}}{\theta_{\text{In}}} = \frac{L-\lambda}{\lambda}. \tag{1}$$

It is explained that varying the mid constraint location directly affects the transmission ratio, exactly like the changes of mechanical advantage when the location of the middle joint of a lever changes. This analogy is illustrated schematically in Fig. 3. In this concept, the warping induced axial displacement of the cross-sections plays the role of the rigid bar in the lever mechanism. It is clear that if we reduce the rigidity of the bar in the lever mechanism, the output/input ratio will not be as ideally expected. A similar logic can explain by the effect of the warping constant on transferring the rotation.

3. Methods

To realize this concept and to understand the effect of warping on the transmission behavior of the proposed mechanism, three open thin-walled cruciform beams are chosen, as shown in Fig. 4. These three beams have the same length (200 mm) and the same web dimensions. However, the flange widths of these three beams are selected to have three sizes as shown in Fig. 4(a). The beams are designed in a way to have torsional constants in the same order of magnitude and warping constants in three different orders of magnitude as shown in Table 1. The warping constant of a cross-section is a measure for the effort needed to reduce warping [24].

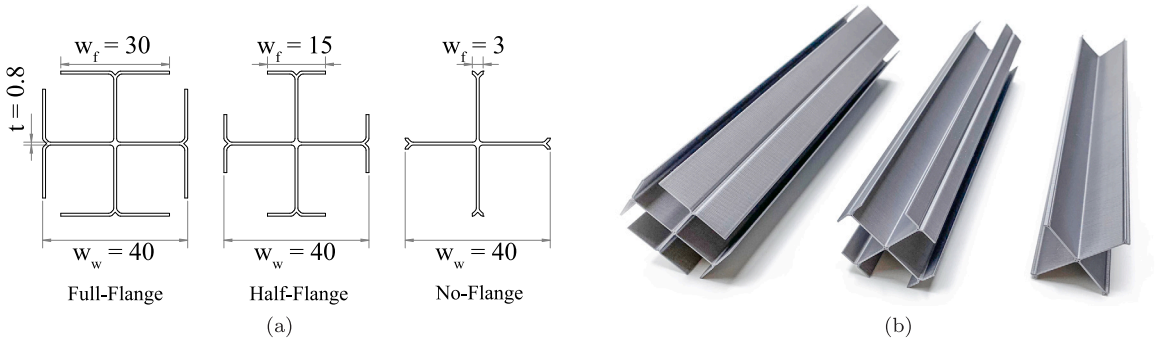

Fig. 4. Three cruciform beams with the same length, same web dimensions, and different flange sizes are chosen to show the effect of warping. (a) shows the dimensions of these beams. (b) shows additive manufactured beams for the experiments.

Table 1
The St. Venant torsional constant (J) and warping constant I_w for three beams with full-flange (w_f = 30 mm), half-flange (w_f = 15 mm), and no-flange (w_f = 3 mm).

	Full-flange	Half-flange	No-flange
J [m^4]	3.48e−11	2.42e−11	1.59e−11
I_w [m^6]	2.76e−12	3.45e−13	3.14e−15

In other words, the effort needed to keep the cross-sections in plane although a torsion is applied. Similarly, the torsional constant of a section is a measure of the effort needed to make an angle of twist in the beam sections.

The warping induced transmission behavior of these beams are analyzed with an analytical solution, FEA with beam and shell elements, and with experiments. The details of each of these methods are described in the following sections.

3.1. Analytical solution

Using Vlasov's torsion theory for beam elements with restrained warping [25], the rotation of a beam cross-section can be derived from this differential equation:

$$m = EI_w \frac{d^4\varphi}{dx^4} - GJ\frac{d^2\varphi}{dx^2}, \tag{2}$$

where GJ is the torsional rigidity, EI_w is the warping rigidity and m is a distributed torsion moment along the beam. The torsion stiffness and warping stiffness are cross-section properties that are obtained using Ansys and shown in Table 1.

The torsion moment can be specified as:

$$M_t = \frac{dB}{dx} + GJ\frac{d\varphi}{dx}, \tag{3}$$

where the bimoment (B) shows the distributions of axial warping induced stress at a cross-section and follows this equation:

$$B = -EI_w\frac{d^2\varphi}{dx^2}. \tag{4}$$

The boundary condition for the beam can be an applied rotation $\varphi = \varphi_0$, or an applied torsion moment $M = M_0$. In this case we imposed an input moment and solved Eq. (2) for each side of the beam. The differential equations were solved using a general form with four boundary conditions for each sides of the beam (eight in total for $x = 0 - C^-$, $x = C^+ - L$) as shown in Fig. 5. The input and output moments and angles can be tweaked separately in this formulation to see the behavior of the beam in different cases. The Matlab code based on this formulation that can solve Eq. (2) with different boundary conditions can be found in the supplementary material.

3.2. Finite Element Modeling (FEM)

The Ansys Parametric Design Language (APDL) has been used to analyze the output to input ratio of the beams. In order to have a fair comparison with the presented analytical formulation and the experiments, two different elements types are used: the beam element as a benchmark for analytical formulation and the more advanced shell element as a benchmark for the experiments.

The material properties of Polylactic Acid (PLA) [26] are used for both the models to match the material of the additive manufactured prototypes. The moments of 0.2 N m and 0.4 N m are exerted on the beam's input side via the ring. The position of the prismatic rotational constraint ring varies in nine steps from −0.06 m to 0.06 m from the middle of the beam $x = 0$ m, to form 1:4 to 4:1 transmission ratios between output and input rotations.

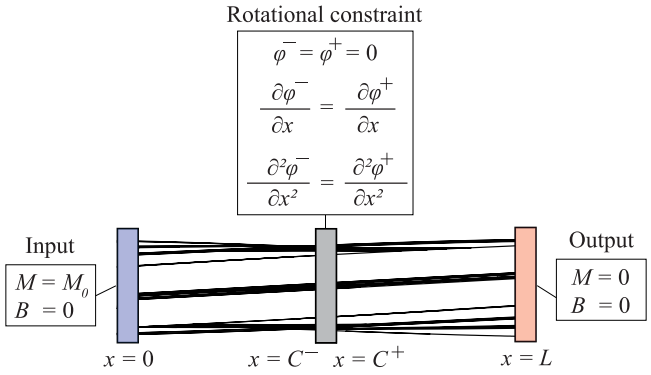

Fig. 5. The boundary conditions of the beam which are used to solve Eq. (2).

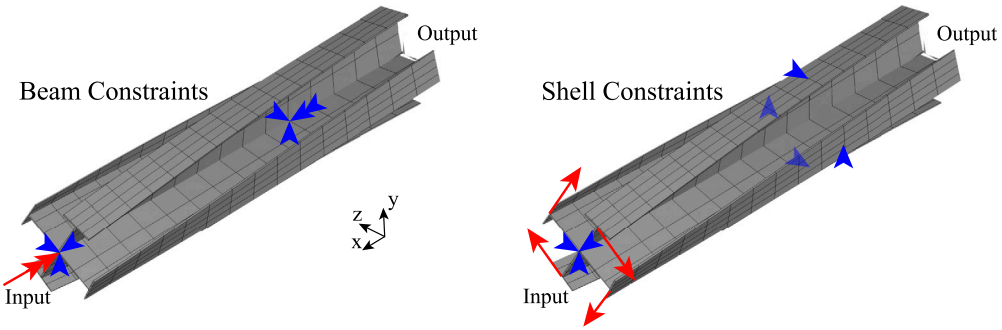

Fig. 6. The model used for the finite element analysis and the rotational constraints imposed on it for both shell and beam elements. Blue arrows are showing constraints, and red arrows are showing input loads and moments. (For interpretation of the references to color in this figure legend, the reader is referred to the web version of this article.)

3.2.1. Beam modeling

To have an estimation of the sectional rotations along the beam to compare with the results from analytical model, the beam element (beam 188) is used. This beam model is based on Timoshenko [27] with warping adapted from Schulz and Filippou [28].

Twenty elements were used to construct the beam. Based on the convergence check, this number of elements is slightly more than what is needed. Also, having 20 elements can give key points on the locations that are important for limiting the rotation for different transmission ratios, which is shown in this work. The beam's input constrained in three translational directions. For the middle ring, two translations, in y and z directions, and one rotation in x direction are implemented as shown in Fig. 6.

3.2.2. Shell modeling

The eight-node shell element (shell 281) is selected as the constructing element. The beam constrained at two positions, one at the input section similar to the beam, and four at the location of the prismatic rotational constraint at the tips of the webs, where points are tangentially constrained as shown in Fig. 6. It is important to note that the shear center of a bi-symmetric cruciform beam is in its center, and ideally the four webs will not warp, considering their small thickness. Therefore, the best location to constrain the rotation is the webs endpoint where there will be in principle no out of plane deformation of the cross-section due to the warping.

The input moment is applied via another set of four points on the input side, where tangential forces are applied. The input and output rotations upon exerted moments are obtained by tracking the rotation of the shear center of the input and output sections.

3.3. Experimental setup

The compliant beams are used as rotation–rotation transmission. Therefore, to have control over the rotations of the sections and to replicate the same constraints described in the FEM, four longitudinal notches are made on the edge of the beam webs, and prismatic rigid rings with four V-shaped keys are designed to fit into these grooves as shown in Fig. 2 and realized in Fig. 7. Putting moments on these rings or constraining them has the same constraining effect described in the FEM for sets of four section-mate points (Fig. 6).

The input ring is constrained in x, y and z directions and a force couple is exerted on it by two ropes connected to suspended weights via pulleys. The applied moment is kept constant as the ropes are wrapped around a central pulley. The moments are

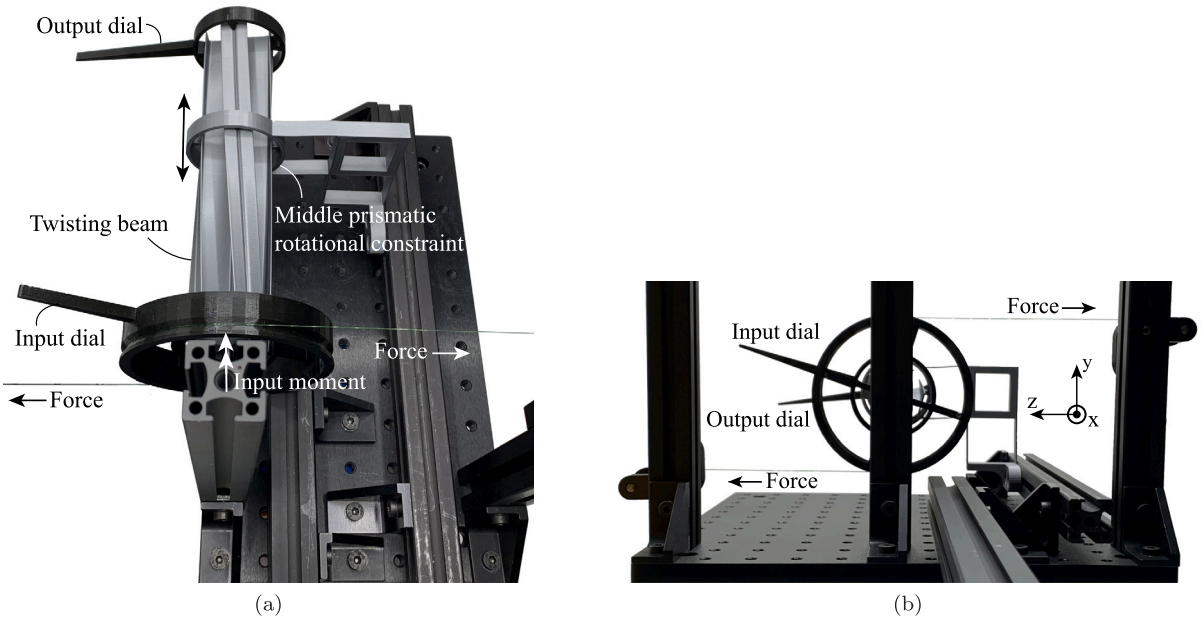

Fig. 7. (a) shows the experimental setup. The beam is constrained in the middle where the compliant *yz* stage allows for translations while constraining the *x* rotation. The input ring is hinged to the ground and a force couple is exerted on it to make an input moment. Input and output rings have dials for image processing of their angles. (b) shows an example of the view which is used in image processing to measure the input and output rotations.

Table 2
The average match rate to ideal ratio for different cross-sections from analytical solution, FEM with beam and shell elements and experiments are shown for beams with the input moments of 0.2 N m and 0.4 N m.

Input Moment [N m]	Full-flange		Half-flange		No-flange	
	0.2	0.4	0.2	0.4	0.2	0.4
Analytical [%]	97	97	86	86	16	14
FEM beam [%]	96	97	86	86	16	16
FEM shell [%]	93	91	79	75	17	16
Experiments [%]	68	67	56	55	10	9

0.2 N m and 0.4 N m. The output ring is free in all directions. The middle constraint ring is connected to an *yz* compliant stage in order to have all freedom except rotation around the *x* axis. This compliant *yz* stage is connected to a slider parallel to the beam's longitudinal direction *x*, so that the middle ring can be moved along the beam. The prismatic motion of this ring can continuously vary the output/input ratio.

The behavior of the beams is examined by experiments on additive manufactured prototypes made out of PLA and shown in Fig. 4(b). The position of the middle constraint ring changes in the same nine steps as described in Section 3.2. The output and input rotation angles are measured by image processing of the output and input dials, which are connected to the rings. An example of an image from which angles are extracted from is shown in Fig. 7(b).

4. Results

To understand how warping induced displacements can transfer the rotation, the nodal rotations (φ) and the nodal warping ($d\varphi/dx$) along all three beams from the analytical solution and from FEM with a beam model are shown in Fig. 8. In this figure an input rotation of 0.5 rad is applied on one side of the beam and the rotational constraint located at the middle of the beam (x= 0.1 m) which is indicated by a vertical line.

Beside the nodal solutions, the output/input rotation and moment are measured to evaluate how close these beam can perform to the ideal ratio from (Eq. (1)). This ideal ratio is shown with a dotted line in Fig. 9 and the ratios which were achieved from beams are shown with colors. The data points are shown with circles and connected to each other with straight lines to show the trend. The resulting ratios are for the output/input rotation, in other words the geometrical advantage in Fig. 9. These results are obtained using the analytical model using an input moment of 0.2 N m.

The match rate to the ideal ratio is a good indicator of how good each of these beams can transfer the motion in different ratios of transmission. Therefore, this match rates with ideal ratio are shown in Fig. 10 for all modeling methods.

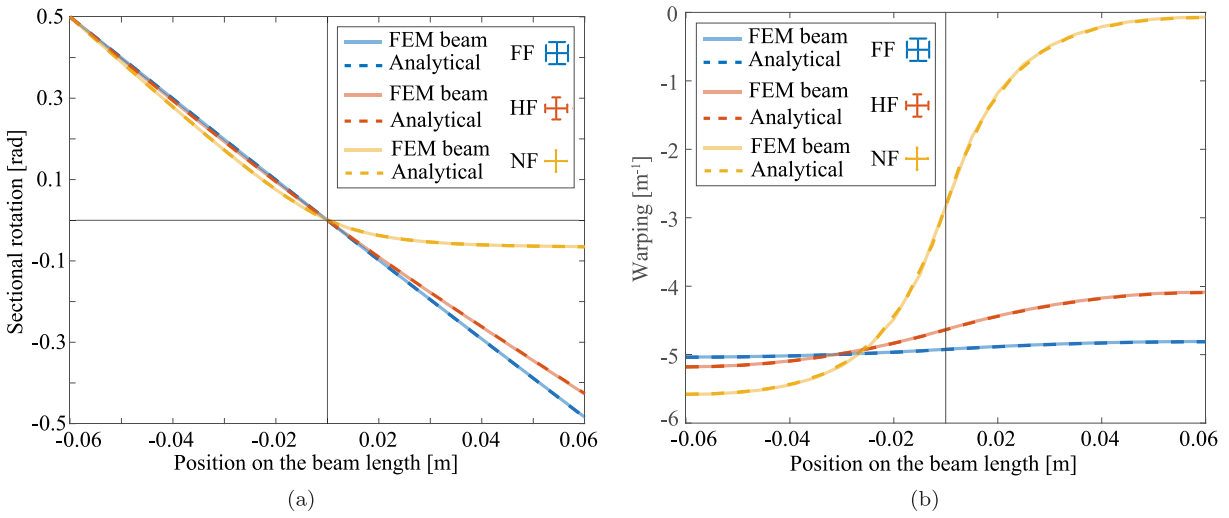

Fig. 8. (a) shows the sectional rotation (φ), and (b) shows the sectional warping ($\mathrm{d}\varphi/\mathrm{d}x$). Both parameters are illustrated for nodes along the three beams when an input rotation of 0.5 rad is applied at the input for a 1:1 ratio. The dashed lines are from the analytical solution and the solid lines are from the FEM with beam elements. (For interpretation of the references to color in this figure legend, the reader is referred to the web version of this article.)

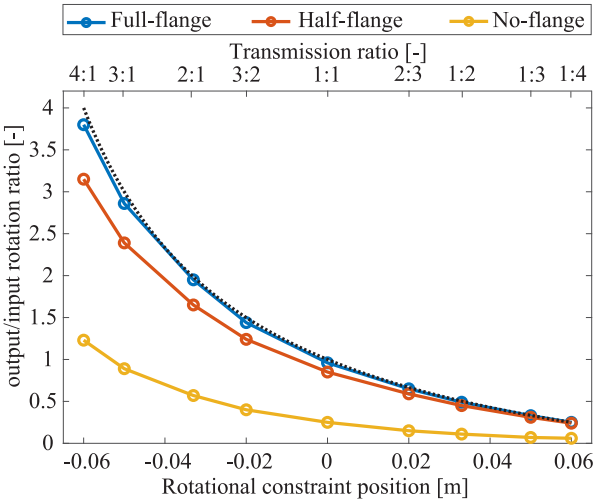

Fig. 9. Resulting output/input angle ratios from analytical solution for the beams with nine different positions of the rotational constraint along the beam are compared with the ideal ratio of Eq. (1). (For interpretation of the references to color in this figure legend, the reader is referred to the web version of this article.)

Another effective parameter that can have effect on the match rate with ideal ratio is the input rotation caused by the input moment. To evaluate this effect all beams undergo input moments ranging from 0.1 N m to 3 N m and the match rates in 1:1 ratio from FEM with shell elements are shown in Fig. 11.

It is mentioned that the experiments and FEM both are performed with 0.2 N m and 0.4 N m as input moments. To have a second insight on the effect of the input moment on the match rate besides Fig. 11, the average match rates from all methods and for these two input moments are indicated in Table 2.

Lastly, in Table 3 an important feature of the transmission is shown, which is the ability to transfer moments while there is a resistant moment on the output. This table shows the resulting ratios between the output and input moments of the full-flange beam while the output resistance increases from 0.5 to 5 N.m. This is shown for geometric transmission ratios of 4:1, 1:1, and 1:4. Fig. 12 illustrates the sectional rotations along the full-flange beam when the resistance increases from 0 to 5 N.m in ten steps for the same ratios that are mentioned in Table 3. It is clear that with higher resistance, the transferred rotation angles decrease, the lines start to deviate from being straight, and the geometrical match rates drop.

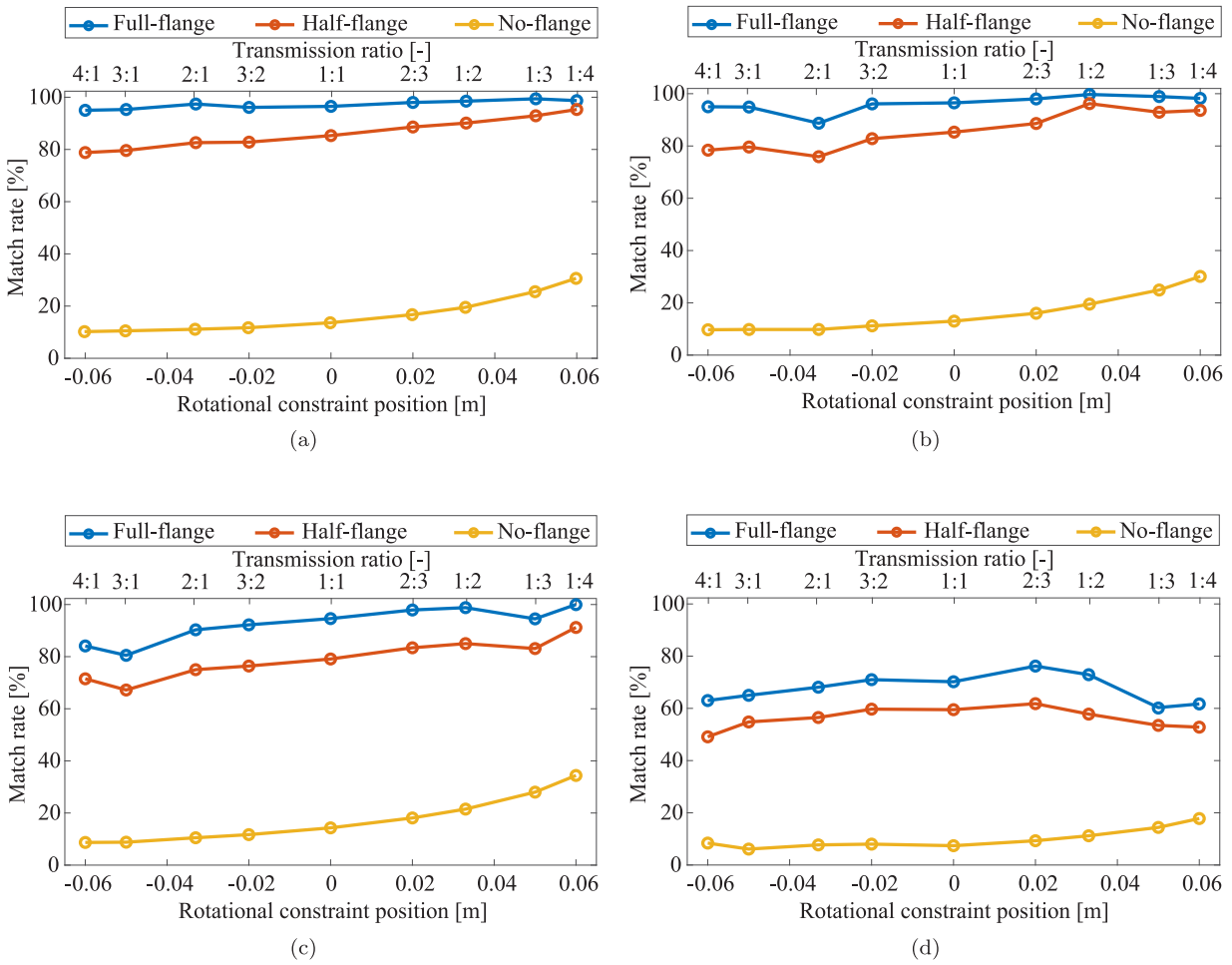

Fig. 10. The geometrical match rates with ideal ratio from Eq. (1) are shown for nine different transmission ratios. The results are obtained from (a) Analytical solution, (b) FEM with beam elements, (c) FEM with shell elements, and (d) Experiments. (For interpretation of the references to color in this figure legend, the reader is referred to the web version of this article.)

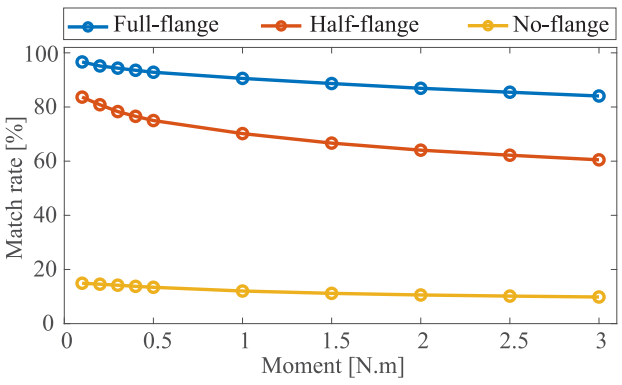

Fig. 11. The effect of input moment on the geometrical match rate for three beams. The results are obtained from the FEM with shell elements with 1:1 ratio. (For interpretation of the references to color in this figure legend, the reader is referred to the web version of this article.)

Table 3
The resulting M_{out}/M_{in} ratios from analytical formulation when the output resistant moment increases from 0.5 to 5 N m for the ideal geometrical ratios of 4/1, 1/1 and 1/4 of the full-flange beam.

	Output resistant moment M_{out} [N m]									
	0.5	1	1.5	2	2.5	3	3.5	4	4.5	5
Ideal ratio	Resulting ratio M_{out}/M_{in} [–]									
4/1	1.77	2.47	2.84	3.07	3.22	3.34	3.42	3.49	3.55	3.59
1/1	0.57	0.73	0.81	0.85	0.88	0.90	0.92	0.93	0.94	0.95
1/4	0.11	0.16	0.18	0.20	0.21	0.22	0.22	0.23	0.23	0.23

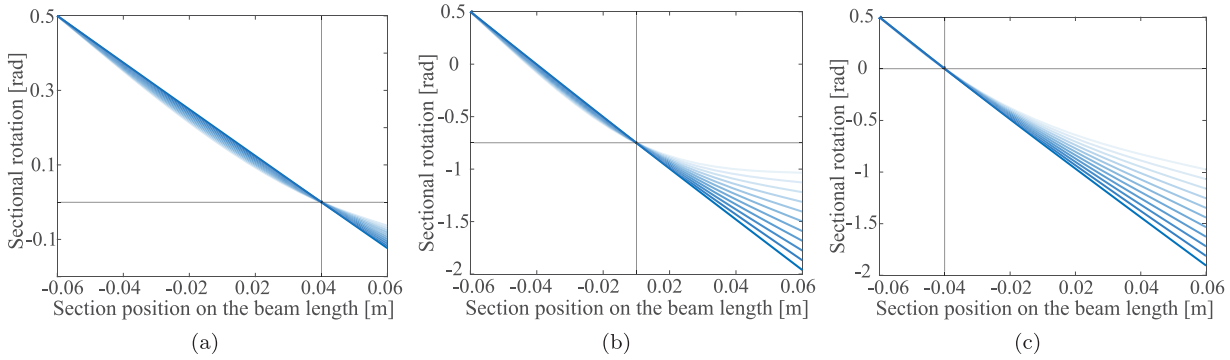

Fig. 12. Effect of output resistant moment on the deviation of sectional twist angles along the beam from the expected uniform twist angle (straight line) when the resistant moment increases from 0 N.m (dark blue) to 5 N.m (light blue) for the full-flange beam for (a) 4/1 ratio, (b) 1/1 ratio, and (c) 1/4 ratio. (For interpretation of the references to color in this figure legend, the reader is referred to the web version of this article.)

5. Discussion

It is shown that warping is a key feature in this transmission. Thus, beams with higher warping constants performed well, while beams with almost no warping could barely transfer any rotation or moment (see Figs. 8 and 9). Moreover, it is also shown that the transmission ratio and the input moment do not have a major effect on the mechanism's match rate and, therefore, on this transmission behavior (almost straight lines in Fig. 10 for all ratios).

The relation between warping constant and achievable match rate is investigated and shows the same trends from all methods. The role of the warping constant in transmission is clear. However, the exact relation between these two can be further investigated, as the full-flange and half-flange beams show close match rates despite the order of magnitude difference in their warping constant (see Fig. 10).

The average match rates from analytical solutions and FEM with the beam element are very close (see Fig. 10a and b). This indicates that the proposed analytical formulation is reliable. The small deviation can be due to the different theories that are utilized in these two models. The results from the beam-based model are close to the results from the more advanced and accurate FEM with shell elements (see Fig. 10b and c). The experiments show the same overall trend, with an average 17% lower match rate compared with FEM with shell elements (see Fig. 10 c and d). This can be due to different mismatches: Firstly, it is not possible to have exactly the same point-constraints on the beam in reality as in the models. Instead, we used prismatic grooves, which are a simple solution but can cause mismatches between experiments and models. Furthermore, some parts of the experimental setup are not infinitely stiff, meaning that they might cause some deformation and, therefore, errors. Secondly, the prototypes were made by additive manufacturing, which causes anisotropy in the structure, this anisotropy was not modeled in FEM and cannot be considered in the beam formulation. Therefore, it can be a major source of discrepancy. Thirdly, the measurement using vision processing can have an error of up to 0.5 degrees, which can cause an error of up to 10% in some measurements with small angles. Fourthly, having small fillets in the connection points of webs and flanges for better bonding and printing results of the prototypes, are not included in any of the models, which can be another source of the mismatch. Fifthly, some assumptions in the models, i.e., no deformations in cross-section shape in the beam model and thin-walled assumptions in the shell model, are not fully true in this case, which means that the models are not completely capturing all the deformations. Using a solid element can capture all these effects and results in better results. However, it will significantly increase the computational cost.

Finally, using PLA as the material for the prototype and having large elastic deformations and large local strains can make material non-linearity a non-negligible factor, which was not considered in any of the used models. As for the use of other materials in a practical embodiment of the presented concept it can be noted that the elastic material parameters such as the Young's Modulus and the Shear Modulus, which relate the moments and the rotation in a linear fashion, have no influence on the kinematic behavior of the transmission. It means that any other linearly elastic material with similarly scaled elastic moduli will have the same input–output behaviors in the unloaded condition. As for the strength parameters such as the yield stress, it is evident that they directly

affect the range of motion of the transmission. Therefore the material strength should be carefully considered in relation to the intended range of motion within the application.

Using a compliant mechanism in this design led to several advantages. However, there are also disadvantages to this type of mechanism. An inherent drawback of compliant mechanisms is that they require energy for deformation. Thus, the output to input energy efficiency of the mechanism becomes lower. It is possible to reduce this elastic strain energy since it is not lost but only temporarily stored in the form of elastic deformation; therefore, by the introduction of prestress, we can compensate for it and store the required energy in the mechanism so that we have a neutrally stable compliant element. This idea is currently being investigated by the authors to enhance the efficiency of the current compliant transmission.

It can be seen in Table 3 and Fig. 12 that for larger amounts of resistant moment, the output over input moment ratio matches closer with the ideal geometric ratio. However, by increasing the resistance, the deviation from a uniform twist angle along the structure increases, which means that the output/input match rate with the ideal geometric ratio drops.

This mechanism is presented mainly for applications where kinematics is the main focus. It is shown that it can transfer the moment as well as the rotation. However, having proportionally high moments at the output can change the warping behavior to semi-restrained and lead to a different mode of deformation where the geometrical transmission may vanish. Nonetheless, it is still possible to analyze and characterize these highly restrained beams with the presented methods.

6. Conclusion

We have presented a design for a CVT using a compliant mechanism. It is shown that the warping induced displacement in the beams with a high warping constant can transfer the rotation from one side to the other, while continuously variable transmission ratios between the sides of the twisting beam can be achieved by the relocation of a prismatic rotational constraint along the beam.

The concept has been explained and investigated using analytical models, finite element analysis, and experiments. The results were compared with an ideal transmission to show the performance of the beams with different warping constants. All methods verified the hypothesized relation between the warping constant and transmission behavior.

More than 90% match rate with an ideal transmission was observed for a non-optimized design from the models. The match rate for the same beam is shown to be above 60% for the transmission ratio between 1:4 and 4:1 in the experiments. This shows the effectiveness and capability of this design. It is possible to further improve this match rate and thus the functionality of the transmission by optimizing the beam parameters.

This concept can be used instead of traditional CVTs in applications where it is essential for the design to be lightweight (e.g., flapping micro-robots, bio-mimetic walking robots), monolithic (e.g., submerged systems), free of backlash (e.g., precision systems and measurement devices), and easy to make on a small scale (e.g., MEMS, metamaterials). However, for applications where a continuous rotation is needed and/or a large amount of power should be transmitted with minimum loss of energy, the state-of-the-art belt and chain CVTs that are introduced in Section 1 can perhaps perform better.

Declaration of competing interest

The authors declare that they have no known competing financial interests or personal relationships that could have appeared to influence the work reported in this paper.

Data availability

Data will be made available on request.

Acknowledgment

This work was supported by the Dutch Research Council (NWO) [P16-05 Shell-Skeletons].

Appendix A. Supplementary data

Supplementary material related to this article can be found online at https://doi.org/10.1016/j.mechmachtheory.2023.105281.

References

[1] G. Carbone, L. Mangialardi, G. Mantriota, A comparison of the performances of full and half toroidal traction drives, Mech. Mach. Theory 39 (9) (2004) 921–942.
[2] K. Atallah, J. Wang, S.D. Calverley, S. Duggan, Design and operation of a magnetic continuously variable transmission, IEEE Trans. Ind. Appl. 48 (4) (2012) 1288–1295.
[3] N. Srivastava, I. Haque, A review on belt and chain continuously variable transmissions (CVT): Dynamics and control, Mech. Mach. Theory 44 (1) (2009) 19–41.
[4] L.L. Howell, S.P. Magleby, B.M. Olsen, Handbook of Compliant Mechanisms, first ed., Wiley, Somerset, 2013.
[5] C. Zhang, C. Rossi, A review of compliant transmission mechanisms for bio-inspired flapping-wing micro air vehicles, Bioinspiration Biomim. 12 (2) (2017) 025005.

[6] S.L. Weeke, N. Tolou, G. Semon, J.L. Herder, A fully compliant force balanced oscillator, in: International Design Engineering Technical Conferences and Computers and Information in Engineering Conference, Vol. 50152, American Society of Mechanical Engineers, 2016, V05AT07A008.
[7] S.H. Collins, M. Wisse, A. Ruina, A three-dimensional passive-dynamic walking robot with two legs and knees, Int. J. Robot. Res. 20 (7) (2001) 607–615.
[8] S. Seok, A. Wang, M.Y. Chuah, D. Otten, J. Lang, S. Kim, Design principles for highly efficient quadrupeds and implementation on the MIT Cheetah robot, in: 2013 IEEE International Conference on Robotics and Automation, IEEE, 2013, pp. 3307–3312.
[9] R. Mak, A. Amoozandeh Nobaveh, G. Radaelli, J.L. Herder, A curved compliant differential mechanism with neutral stability, in: International Design Engineering Technical Conferences and Computers and Information in Engineering Conference, American Society of Mechanical Engineers, 2022.
[10] J.B. Hopkins, R.M. Panas, Design of flexure-based precision transmission mechanisms using screw theory, Precis. Eng. 37 (2) (2013) 299–307.
[11] D.F. Machekposhti, N. Tolou, J. Herder, A statically balanced fully compliant power transmission mechanism between parallel rotational axes, Mech. Mach. Theory 119 (2018) 51–60.
[12] C.B. Pedersen, A.A. Seshia, On the optimization of compliant force amplifier mechanisms for surface micromachined resonant accelerometers, J. Micromech. Microeng. 14 (10) (2004) 1281.
[13] T. Okada, K. Tahara, Development of a two-link planar manipulator with continuously variable transmission mechanism, in: 2014 IEEE/ASME International Conference on Advanced Intelligent Mechatronics, IEEE, 2014, pp. 617–622.
[14] L.L. Chu, J.A. Hetrick, Y.B. Gianchandani, High amplification compliant microtransmissions for rectilinear electrothermal actuators, Sensors Actuators A 97 (2002) 776–783.
[15] N.D. Mankame, G.K. Ananthasuresh, A compliant transmission mechanism with intermittent contacts for cycle-doubling, J. Mech. Des. 129 (1) (2006) 114–121.
[16] X. Lachenal, S. Daynes, P.M. Weaver, A non-linear stiffness composite twisting I-beam, J. Intell. Mater. Syst. Struct. 25 (6) (2014) 744–754.
[17] G. Radaelli, Reverse-twisting of helicoidal shells to obtain neutrally stable linkage mechanisms, Int. J. Mech. Sci. 202 (2021) 106532.
[18] D. Farhadi Machekposhti, N. Tolou, J. Herder, A review on compliant joints and rigid-body constant velocity universal joints toward the design of compliant homokinetic couplings, J. Mech. Des. 137 (3) (2015) 032301.
[19] R. Vos, Z. Gürdal, M. Abdalla, Mechanism for warp-controlled twist of a morphing wing, J. Aircr. 47 (2) (2010) 450–457.
[20] M.J. Bianco, A.K. Habtemariam, C. Könke, V. Zabel, Analysis of warping and distortion transmission in mixed shell–GBT (generalized beam theory) models, Int. J. Adv. Struct. Eng. 11 (1) (2019) 109–126.
[21] S. Shayan, K. Rasmussen, A model for warping transmission through joints of steel frames, Thin-Walled Struct. 82 (2014) 1–12.
[22] C. Basaglia, D. Camotim, N. Silvestre, Torsion warping transmission at thin-walled frame joints: Kinematics, modelling and structural response, J. Construct. Steel Res. 69 (1) (2012) 39–53.
[23] M. Valentijn, Thin-walled warping beams for differential mechanism applications, 2020.
[24] P. Hoogenboom, A. Borgart, Method for including restrained warping in traditional frame analyses, Heron 50 (1) (2005).
[25] V. Vlasov, Thin-Walled Elastic Beams, Israel Program for Scientific Translation, Tel Aviv, 1961, English translation. Published for NSF and Dept. of Commerce, USA.
[26] A. Qattawi, B. Alrawi, A. Guzman, et al., Experimental optimization of fused deposition modelling processing parameters: a design-for-manufacturing approach, Procedia Manuf. 10 (2017) 791–803.
[27] S. Timoshenko, Theory of Elastic Stability 2e, Tata McGraw-Hill Education, 1970.
[28] M. Schulz, F.C. Filippou, Generalized warping torsion formulation, J. Eng. Mech. 124 (3) (1998) 339–347.